U. S. Department of Commerce
National Bureau of Standards

Research Paper RP1861
Volume 40, February 1948

Part of the Journal of Research of the National Bureau of Standards

Perforated Cover Plates for Steel Columns; Compressive Properties of Plates Having Ovaloid, Elliptical, and "Square" Perforations

By Ambrose H. Stang and Bernard S. Jaffe

Tests were made to determine the mechanical properties of perforated cover plates intended to be used as a substitute for lattice bars or batten plates in built-up box-type columns. These tests supplement and extend the range of perforation shapes beyond that described in preceding reports.

This paper gives the results for seven plates having perforations of ovaloid shape, six with the long axis parallel to the load, and one with the short axis parallel to the load; three plates having elliptical perforations with the major axis parallel to the load; two plates having square perforations with rounded corners for one of which the load was parallel to the side of the square, and for the other of which the load was parallel to a diagonal. A column having a solid plate was also tested for comparison with the columns having perforated plates.

Tests were made to determine the stiffness of the perforated plate columns relative to that of the column having a solid plate, the distribution of stress on the edge of the perforation, and the strength of each column.

I. Introduction

This paper is the seventh of a series dealing with the experimental determination of the mechanical properties of perforated cover plates intended to be used as a substitute for lattice bars or batten plates in built-up box-type columns. The columns for which the results are here reported are additions to the original program.[1]

In that program, the ratio of perforation width to plate width was 0.45 for nearly all of the perforated plates. In this series, plates with ovaloid perforations with the load parallel to the long axis and having ratios of perforation width to plate width of 0.255 and 0.647 have been included to cover a wider range for this ratio. Plates having elliptical perforations with the major axis parallel to the load, ovaloid perforations with the short axis parallel to the load, "square" perforations with the side of the square in one plate and with the diagonal, in another plate, parallel to the load, have also been included.

II. Cover-Plate Columns

The details of the columns are shown in figures 1 and 2. The columns were riveted before delivery to the laboratory. The ends had been milled after assembly and were reasonably smooth and parallel. A piece of material 20 in. long, which had been cut from each plate and angle used in the columns, was delivered with the columns.

[1] Ambrose H. Stang and Martin Greenspan, J. Research NBS **28**, 609 (1942) RP1473; **28**, 687 (1943) RP1474; **29**, 279 (1942) RP1501; **30**, 15 (1943) RP1514; **30**, 177 (1943) RP1527; **30**, 411 (1943) RP1540.

TABLE 1. *Areas for the columns*

Column	Angle area	Plate area		Column area			
		Gross	Net	Gross, A_g	Net, A_n	Ratio, A_g/A_n	Ratio, A_n/A_g
	*in.*²	*in.*²	*in.*²	*in.*²	*in.*²		
C4D–A	11.454	9.514	9.514	20.968	20.968	1.000	1.000
C4E–1	11.461	9.644	7.138	21.105	18.599	1.135	0.881
C4E–2	11.461	9.644	7.128	21.105	18.590	1.135	.881
C4E–3	11.461	9.644	7.146	21.105	18.608	1.134	.882
C4F–1	11.638	9.677	3.416	21.316	15.054	1.416	.706
C4F–2	11.638	9.677	3.439	21.316	15.077	1.414	.707
C4F–3	11.638	9.677	3.391	21.316	15.029	1.418	.705
C4G–1	11.604	9.707	5.328	21.311	16.932	1.259	.795
C4G–2	11.604	9.707	5.329	21.311	16.933	1.259	.795
C4G–3	11.604	9.707	5.330	21.311	16.935	1.258	.795
C4H	11.630	9.836	5.354	21.466	16.984	1.264	.791
C4I	11.450	9.798	5.350	21.248	16.800	1.265	.791
C4J	11.486	9.831	5.306	21.317	16.792	1.269	.788

The dimensions given in figures 1 and 2 are nominal. There were the usual commercial variations in the thicknesses and widths of the plates. The variations in the dimensions of the perforations were considerably greater; for some plates, the differences between the maximum and minimum perforation length or width as well as the difference from the nominal dimensions was greater than 0.1 in.

As the columns were already riveted when delivered, the cross-sectional areas of the plates and angles of the columns were computed from the dimensions of the extra lengths of material rather than from measurements on the columns.

No distinguishing marks had been placed on the three columns of the same design or on the three extra lengths of material representing them. The dimensions of the extra lengths having the same mark were therefore averaged, and the gross cross-sectional areas of the three columns of the same design were taken as identical.

The cross-sectional areas of the plates and angles and of the columns, computed from the measured dimensions, are given in table 1.

III. Procedure

Coupons representing the plate and angle material were cut in the direction of rolling and tested in tension. Young's modulus of elasticity, Poisson's ratio, the upper and lower yield point, and tensile strength were determined.

A composite sample of the plate material and a composite sample of the angle material were analyzed for carbon, manganese, phosphorus, and sulfur.

The methods used in testing the columns were the same as those described in the references in footnote 1, except as noted below. The shortening under load in the elastic range was determined for each column.

The strains in the edge of the middle perforation were determined for each of the C4E and C4F columns, using a Berry hand-operated strain gage, 2-in. gage length. The values for each of the three similar columns were averaged. The strains in the edge of the middle perforation of columns C4G–2, C4H, C4I, and C4J were measured with Huggenberger tensometers, 1-in. gage length. The stress distribution on the edge of the perforations was calculated from the strain data and the values of Young's modulus obtained from the coupon tests.

Each column was tested to destruction. Data to complete the stress-strain curves and data for the stress-deflection curves were taken.

IV. Results

The average results of the tensile tests of the coupons are given in table 2, and the chemical composition of the coupon material is given in table 3.

The moduli, E', of the columns, and the effective-area factors, K, with respect to shortening under compressive load, for the plates, are given in table 4.[2]

[2] Ambrose H. Stang and Martin Greenspan, J. Research NBS **28**, 679–80 (1942) RP1473.

TABLE 2. *Average results of tensile tests of coupons*

Column designation	No. of coupons	Thickness	Young's modulus	Poisson's ratio	Yield point		Tensile strength
					Upper	Lower	
PLATE COUPONS							
		in.	*kips/in.²*		*kips/in.²*	*kips/in.²*	*kips/in.²*
C4D-A	1	0.372	30,000	0.258	38.5	37.1	62.6
C4E	3	.376	29,900	.263	38.6	37.0	64.2
C4F	3	.378	30,000	.270	39.2	36.5	63.0
C4G	3	.380	29,900	.270	39.3	36.7	62.7
C4H	1	.385	29,500	.259	40.2	37.3	63.7
C4I	1	.382	29,600	.269	38.7	37.2	63.4
C4J	1	.383	29,900	.262	38.6	35.8	62.4
ANGLE COUPONS							
C4D-A	2	0.488	30,000	0.271	48.2	45.7	68.0
C4E	6	.488	29,900	.277	46.6	44.7	67.7
C4F	6	.496	29,200	.262	46.5	44.3	63.5
C4G	6	.496	29,500	.272	47.0	44.2	63.9
C4H	2	.496	29,400	.260	46.7	44.9	63.8
C4I	2	.488	29,800	.276	47.8	45.7	67.3
C4J	2	.486	29,600	.276	47.2	45.6	67.2

TABLE 3. *Chemical composition of coupon material*

Composite sample	Carbon	Manganese	Phosphorus	Sulfur
	Percent	*Percent*	*Percent*	*Percent*
Plates	0.24	0.39	0.010	0.040
Angles	.25	.39	.011	.033

The distribution of stress on the edge of the middle perforation is shown in figures 3, 4, 5, 6, 7, and 8.

The vertical axis of the graph in each figure is a development of one quadrant of the edge of the perforation. In the stress ratios, $\sigma_{u,v}/(P/A_n)$, A_n is the net area of the column, and σ_u and σ_v are the maximum and the minimum principal stresses, respectively.

The maximum stress ratios are given in table 4. The stress ratios based on gross area, $\sigma_{u,v}/(P/A_g)$, where A_g is the gross area of the column, may be calculated from the values in figures 3 to 8, by multiplying those values by the column area ratio, A_g/A_n, of table 1.

The axial shortening of the column was measured using eight compressometers located as shown in figure 7 of Research Paper RP1473.[3] These compressometers had a gage length equal to two bay lengths. The gage-length shortenings thus represented the shortening in the uniformly perforated portion of the plate. The strain for a given load was calculated by dividing the average shortening in the eight gage lengths by the average gage length. The stress-strain graphs for the columns, based on net areas, are shown in figure 9. The stresses on gross area may be obtained by multiplying the stresses on net area by the column area ratio, A_n/A_g, of table 1.

[3] Ambrose H. Stang and Martin Greenspan, J. Research NBS **28**, 679 (1942) RP1473.

TABLE 4. *Moduli of columns, effective area factors of plates, and maximum-stress ratios*

Column designation	Based on gross area			Based on net area		
	Modulus, E'	Effective area factor, K	Ratio, maximum stress, P/A	Modulus, E'	Effective area factor, K	Ratio, maximum stress, P/A
SOLID PLATE						
	kips/in.²			*kips/in.²*		
C4D-A	30,100			30,100		
PERFORATIONS OVALOID; LOAD PARALLEL TO LONG AXIS						
C4E-1	27,800	0.83		31,500	1.12	
C4E-2	27,600	.82		31,300	1.11	
C4E-3	27,800	.83		31,500	1.13	
Avg	27,700	0.83	−2.28	31,400	1.12	−2.01
C4F-1	21,700	0.39		30,800	1.10	
C4F-2	21,800	.40		30,800	1.11	
C4F-3	21,900	.40		31,000	1.14	
Avg	21,800	0.40	−2.39	30,900	1.12	−1.69
PERFORATIONS ELLIPTICAL; LOAD PARALLEL TO MAJOR AXIS						
C4G-1	25,200	0.64		31,700	1.17	
C4G-2	25,100	.64	−2.43	31,600	1.17	−1.93
C4G-3	25,100	.64		31,600	1.16	
Avg	25,100	0.64		31,600	1.17	
PERFORATIONS OVALOID; LOAD PARALLEL TO SHORT AXIS						
C4H	25,200	0.65	−3.94	31,900	1.19	−3.12
PERFORATIONS "SQUARE"; LOAD PARALLEL TO SIDE						
C4I	24,900	0.63	−3.82	31,500	1.15	−3.02
PERFORATIONS "SQUARE"; LOAD PARALLEL TO DIAGONAL						
C4J	25,700	0.69	−9.40	32,600	1.27	−7.41

771185—48——3

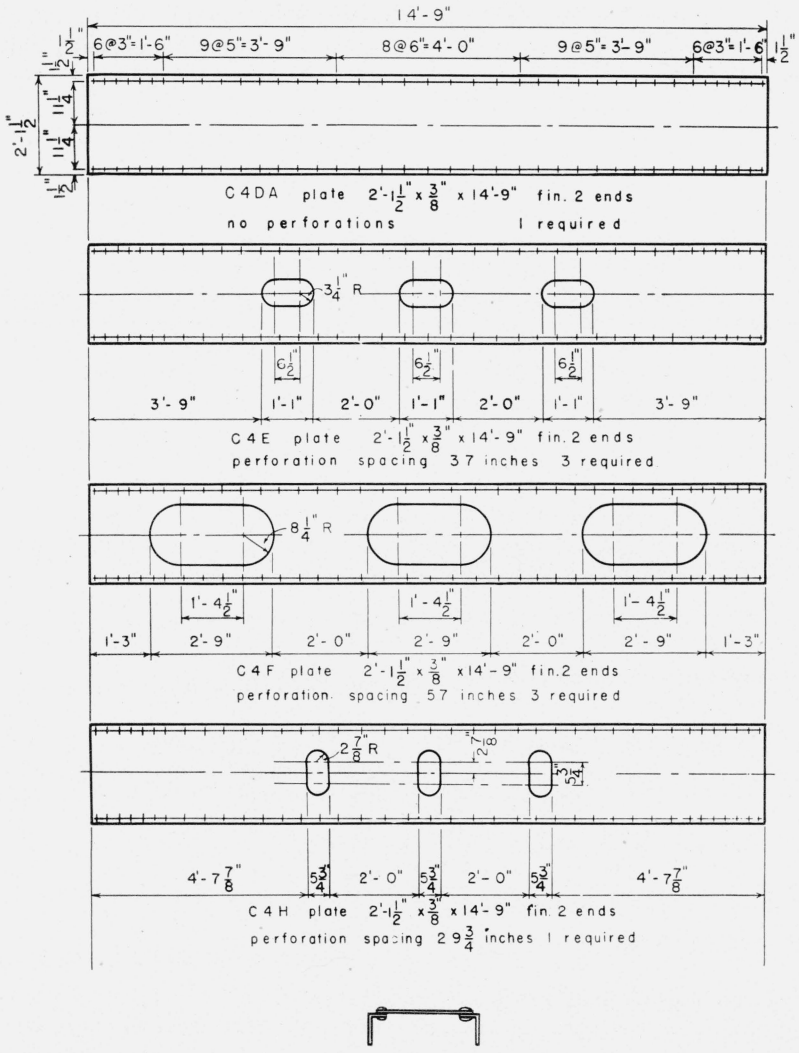

FIGURE 1. *Columns having a solid plate and plates with ovaloid perforations.*

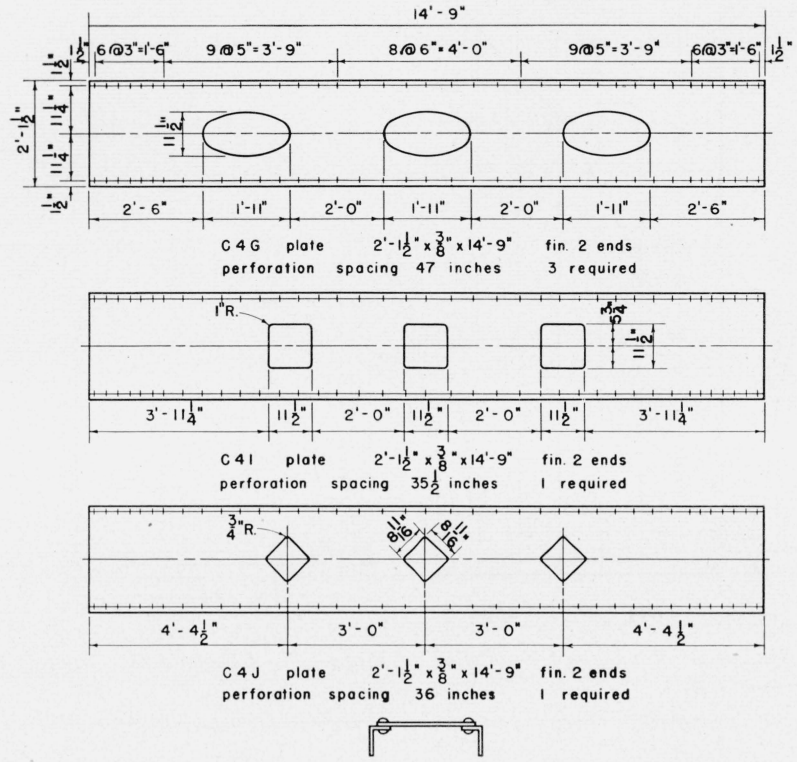

FIGURE 2. *Columns having plates with elliptical perforations and with "square" perforations.*

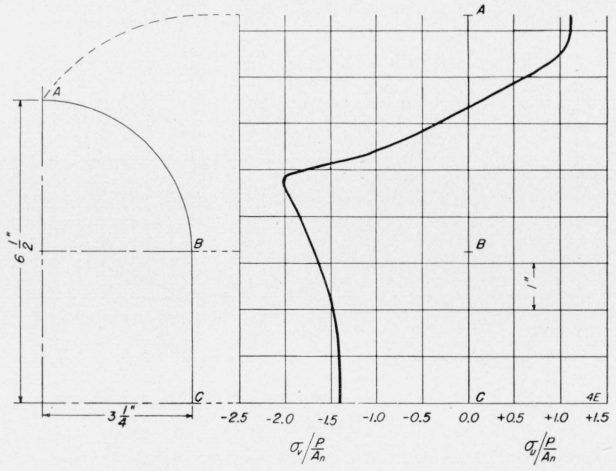

FIGURE 3. *Columns C4E, ovaloid hole, load parallel to long axis.*

Distribution of stress on the edge of the perforation. Based on net area

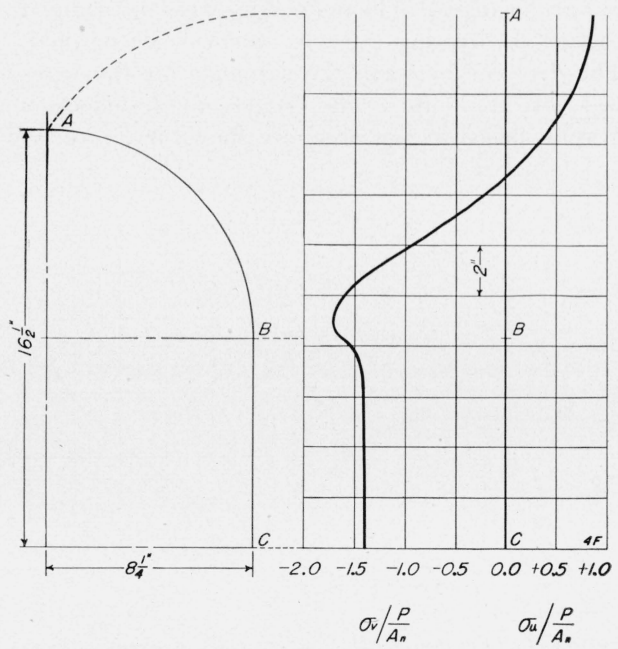

FIGURE 4. *Columns C4F, ovaloid hole, load parallel to long axis.*

Distribution of stress on the edge of the perforation. Based on net area.

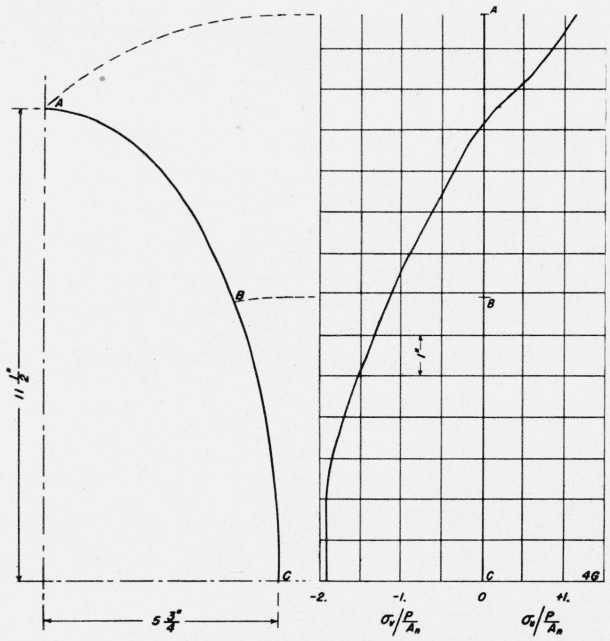

FIGURE 5. *Column C4G–2, elliptical hole, load parallel to major axis.*

Distribution of stress on the edge of the perforation. Based on net area.

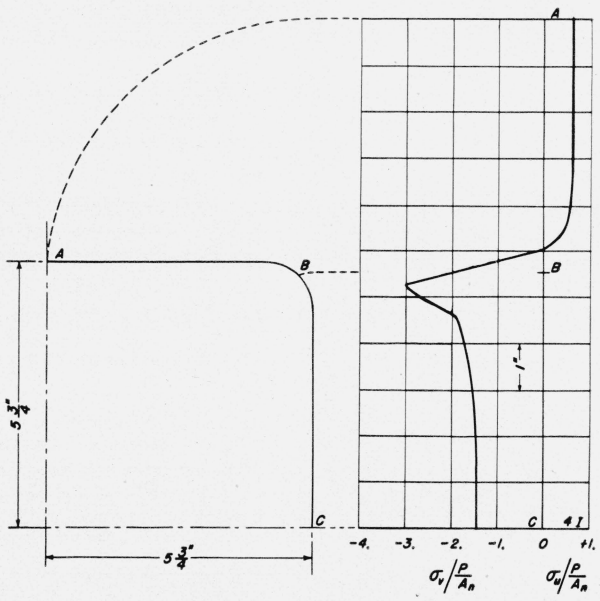

FIGURE 7. *Column C4I, "square" hole, load parallel to side.*

Distribution of stress on the edge of the perforation. Based on net area.

The lateral deflections at midheight of the column, in planes at right angles to the principal axes of inertia of the cross section, were measured at various loads. The deflections were determined to 0.01 in. by the taut-wire mirror-scale method. The distance between the supports for the wires was 14 ft 3 in. The stress-lateral-deflection graphs, based on net area, are shown in figure 10.

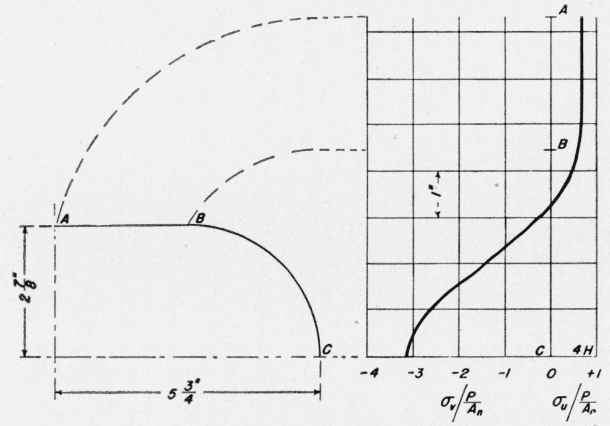

FIGURE 6. *Column C4H, ovaloid hole, load parallel to short axis.*

Distribution of stress on the edge of the perforation. Based on net area.

The maximum loads for the columns, the maximum average stress on the gross area and on the net area, and the effective-area factors [4] of the plates with respect to compressive strength, C, are given in table 5.

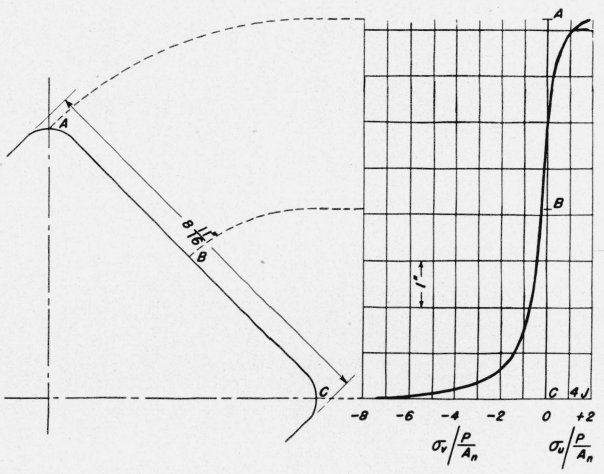

FIGURE 8. *Column C4J, "square" hole, load parallel to diagonal.*

Distribution of stress on the edge of the perforation. Based on net area.

[4] Ambrose H. Stang and Martin Greenspan, J. Research NBS **28**, 685–86 (1942) RP1473.

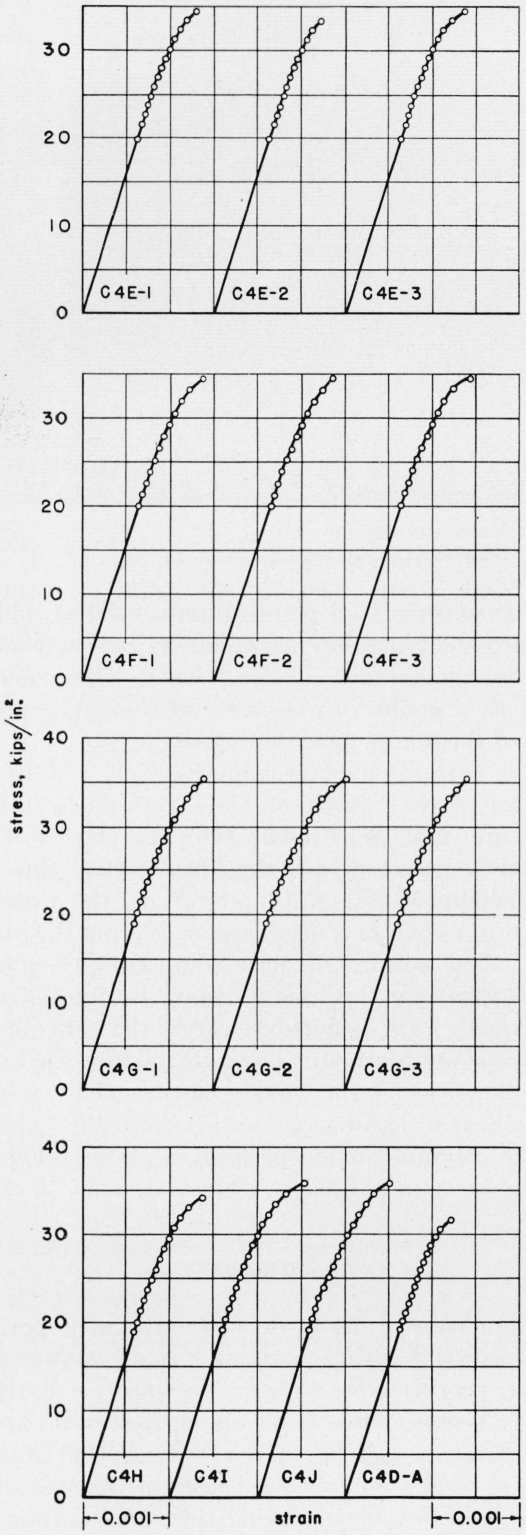

FIGURE 9. *Stress-strain graphs for the columns.*
Based on net area.

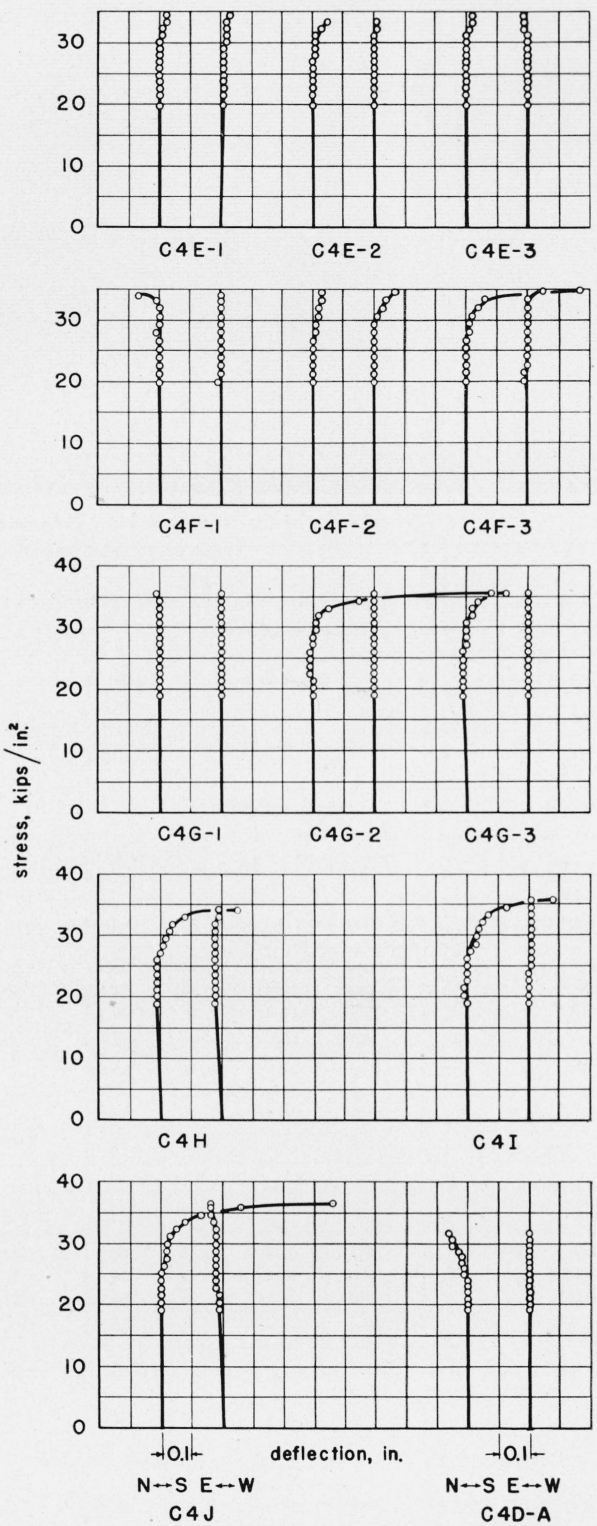

FIGURE 10. *Stress-deflection graphs for the columns.*
Based on net area. When the deflection is north, N, the bending stress is tensile on the plate side.

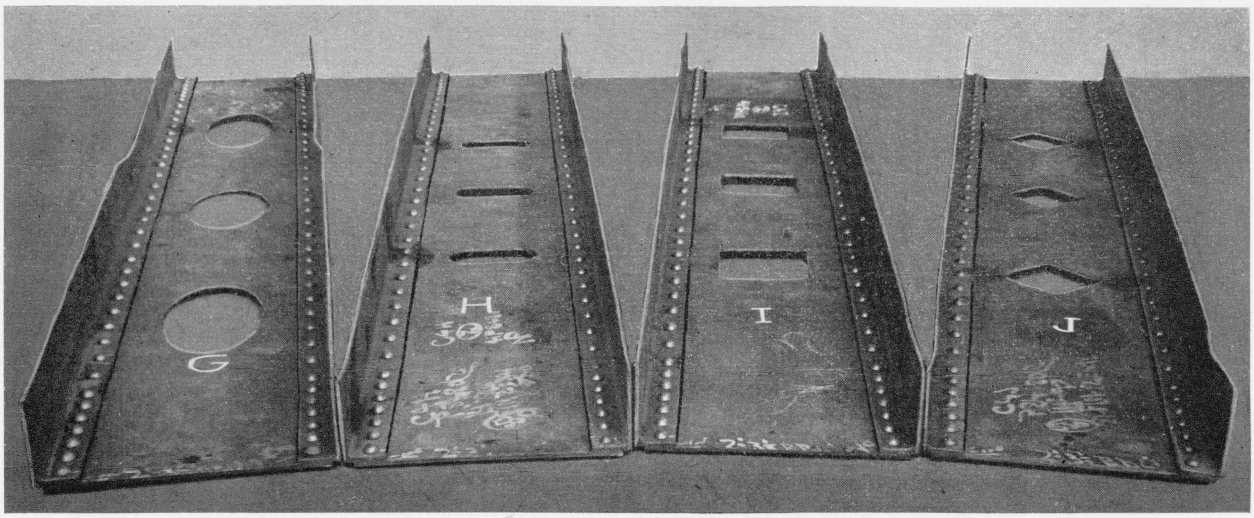

FIGURE 11. *Columns after maximum load tests.*
From left to right, the columns are C4G–1, C4H, C4I, and C4J.

TABLE 5. *Maximum loads for columns and effective area factors for plates*

Column designation	Maximum compressive load	Based on gross area		Based on net area	
		Maximum compressive stress	Effective area factor, C	Maximum compressive stress	Effective area factor, C
SOLID PLATE					
	kips	*kips/in.²*		*kips/in.²*	
C4D-A	678	32.3	1.00	32.3	1.00
PERFORATIONS OVALOID; LOAD PARALLEL TO LONG AXIS					
C4E-1	659	31.2	0.93	35.4	1.25
C4E-2	630	29.9	.83	33.9	1.13
C4E-3	655	31.0	.91	35.2	1.23
Aug	648	30.7	0.89	34.8	1.20
C4F-1	525	24.6	0.48	34.9	1.35
C4F-2	538	25.2	.52	35.7	1.45
C4F-3	520	24.4	.46	34.6	1.31
Avg	528	24.7	0.49	35.1	1.37
PERFORATIONS ELLIPTICAL; LOAD PARALLEL TO MAJOR AXIS					
C4G-1	613	28.8	0.76	36.2	1.38
C4G-2	600	28.2	.72	35.4	1.31
C4G-3	610	28.6	.75	36.0	1.36
Avg	608	28.5	.74	35.9	1.35
PERFORATIONS OVALOID; LOAD PARALLEL TO SHORT AXIS					
C4H	581	27.1	0.64	34.2	1.18
PERFORATIONS "SQUARE"; LOAD PARALLEL TO SIDE					
C4I	600	28.2	0.73	35.7	1.33
PERFORATIONS "SQUARE"; LOAD PARALLEL TO DIAGONAL					
C4J	610	28.6	0.75	36.3	1.39

The unperforated plate column, C4D–A, failed toward the plate side as would be expected from the double modulus column theory. The column bent as a whole with buckling of the outstanding legs of the angles near midheight.

The perforated plate columns, C4E–1, C4E–2, C4E–3, C4F–2, C4F–3, C4G–2, C4G–3, C4H, C4I, and C4J, failed away from the plate side as would be expected from the consideration that, in the neighborhood of a perforation, the gravity axis of the column is displaced away from the plate side. The perforated plate columns, C4F–1 and C4G–1, failed in the other direction, having suffered practically no deflection until the maximum load was approached. Local buckling of the outstanding legs of the angles and buckling of the plate near a perforation characterized the failures of the columns having perforated plates. Figure 11 shows columns C4G–1, C4H, C4I, and C4J after test.

V. Summary

The results of the tests of the columns reported here, as well as of the perforated plate columns for which properties have been previously reported, will be discussed in a forthcoming Research Paper. Comparisons will be made between the experimental results and values based on theories that have been developed during this investigation.

WASHINGTON, October 13, 1947.